INTERNATIONAL STANDARD

ISO 20998-3

First edition
2017-04

Measurement and characterization of particles by acoustic methods —

Part 3: Guidelines for non-linear theory

Mesurage et caractérisation des particules par des méthodes acoustiques —

Partie 3: Lignes directrices pour la théorie non linéaire

Reference number
ISO 20998-3:2017(E)

ISO copyright office
Ch. de Blandonnet 8 • CP 401
CH-1214 Vernier, Geneva, Switzerland
Tel. +41 22 749 01 11
Fax +41 22 749 09 47
copyright@iso.org
www.iso.org

Contents

Page

Foreword

ISO (the International Organization for Standardization) is a worldwide federation of national standards bodies (ISO member bodies). The work of preparing International Standards is normally carried out through ISO technical committees. Each member body interested in a subject for which a technical committee has been established has the right to be represented on that committee. International organizations, governmental and non-governmental, in liaison with ISO, also take part in the work. ISO collaborates closely with the International Electrotechnical Commission (IEC) on all matters of electrotechnical standardization.

The procedures used to develop this document and those intended for its further maintenance are described in the ISO/IEC Directives, Part 1. In particular the different approval criteria needed for the different types of ISO documents should be noted. This document was drafted in accordance with the editorial rules of the ISO/IEC Directives, Part 2 (see www.iso.org/directives).

Attention is drawn to the possibility that some of the elements of this document may be the subject of patent rights. ISO shall not be held responsible for identifying any or all such patent rights. Details of any patent rights identified during the development of the document will be in the Introduction and/or on the ISO list of patent declarations received (see www.iso.org/patents).

Any trade name used in this document is information given for the convenience of users and does not constitute an endorsement.

For an explanation on the voluntary nature of standards, the meaning of ISO specific terms and expressions related to conformity assessment, as well as information about ISO's adherence to the World Trade Organization (WTO) principles in the Technical Barriers to Trade (TBT) see the following URL: www.iso.org/iso/foreword.html .

This document was prepared by Technical Committee ISO/TC 24, *Particle characterization including sieving*, Subcommittee SC 4, *Particle characterization*.

A list of all the parts in the ISO 20998 series can be found on the ISO website

Introduction

Ultrasonic spectroscopy is widely used to measure particle size distribution (PSD) in colloids, dispersions, and emulsions[1][2][3][4]. The basic concept is to measure the frequency-dependent attenuation and/or velocity of the ultrasound as it passes through the sample. This attenuation includes contributions due to scattering or absorption by particles in the sample, and the size distribution and concentration of dispersed material determines the attenuation spectrum[5][6][7]. Once this connection is established by empirical observation or by theoretical calculations, one can estimate the PSD from the ultrasonic data.

Ultrasonic techniques are useful for dynamic online measurements in concentrated slurries and emulsions. Traditionally, such measurements have been made offline in a quality control lab, and constraints imposed by the instrumentation have required the use of diluted samples. By making in-process ultrasonic measurements at full concentration, one does not risk altering the dispersion state of the sample. In addition, dynamic processes (such as flocculation, dispersion, and comminution) can be observed directly in real time [8]. This data can be used in process control schemes to improve both the manufacturing process and the product performance.

Measurement and characterization of particles by acoustic methods —

Part 3:
Guidelines for non-linear theory

1 Scope

This document gives guidelines for ultrasonic attenuation spectroscopy methods for determining the size distributions of one or more material phases dispersed in a liquid at high concentrations, where the ultrasonic attenuation spectrum is not a linear function of the particle volume fraction. In this regime, particle-particle interactions are not negligible.

This document is applicable to colloids, dispersions, slurries, and emulsions. The typical particle size for such analysis ranges from 10 nm to 3 mm, although particles outside this range have also been successfully measured. Measurements can be made for concentrations of the dispersed phase ranging from about 5 % by volume to over 50 % by volume, depending on the density contrast between the continuous and the dispersed phases, the particle size, and the frequency range[9] [10]. These ultrasonic methods can be used to monitor dynamic changes in the size distribution, including agglomeration or flocculation.

2 Normative references

The following documents are referred to in the text in such a way that some or all of their content constitutes requirements of this document. For dated references, only the edition cited applies. For undated references, the latest edition of the referenced document (including any amendments) applies.

ISO 14488:2007, *Particulate materials — Sampling and sample splitting for the determination of particulate properties*

ISO 20998-1:2006, *Measurement and characterization of particles by acoustic methods — Part 1: Concepts and procedures in ultrasonic attenuation spectroscopy*

ISO 20998-2:2013, *Measurement and characterization of particles by acoustic methods — Part 2: Guidelines for linear theory*

3 Terms and definitions

For the purposes of this document, the terms and definitions given in ISO 20998-1 and ISO 20998-2 apply.

ISO and IEC maintain terminological databases for use in standardization at the following addresses:

— ISO Online browsing platform: available at http://www.iso.org/obp

— IEC Electropedia: available at http://www.electropedia.org/

4 Symbols and abbreviated terms

For the purposes of this document, the following symbols and abbreviated terms apply.

a	particle radius
c, c'	speed of sound in the liquid and particle, respectively
C_P	specific heat at constant pressure
CV	coefficient of variation (ratio of the standard deviation to the mean value)
d	average distance between adjacent particles
dB	decibel
e	base of the natural logarithm
ECAH	Epstein-Carhart-Allegra-Hawley (theory)
f	frequency
G	real part of the effective coupling parameter S
i	the imaginary number
k	complex wavenumber
M	radius of shell in core-shell model
PSD	particle size distribution
R	imaginary part of the effective coupling parameter S
S	complex number representing the effective coupling between fluid and particle
SNR	ratio of signal level to noise level
x	particle diameter
x_{10}	the 10th percentile of the cumulative PSD
x_{50}	median size (50th percentile)
x_{90}	the 90th percentile of the cumulative PSD
$\boldsymbol{\alpha}$	attenuation spectrum
β, β'	compressibility of the liquid and particle, respectively
$\bar{\beta}$	mean compressibility of the slurry
δ_T	thermal wave skin depth
δ_V	viscous wave skin depth
η	viscosity of the liquid
κ	thermal conductivity
ρ, ρ'	density of the liquid and particle, respectively
$\bar{\rho}$	mean density of the slurry
ρ^*	mean density at the complementary concentration (1-ϕ)

ϕ volume concentration of the dispersed phase

ϕ_m maximum volume concentration of the dispersed phase (maximum packing)

ϕ_{NL} concentration at which the skin depth becomes equal to the interparticle distance

ω angular frequency (i.e. 2π times the frequency)

5 Limits of applicability of linear theory

5.1 Multiple scattering

The interaction of a plane compressional sound wave with a particle generates three waves propagating outward: 1) a compressional wave; 2) a thermal wave; and 3) a viscous (transverse) wave. The thermal and viscous waves propagate only a short distance (of the order of 0,5 μm in water at 1 MHz) through the liquid.

In the linear model (discussed in ISO 20998-2), attenuation is directly proportional to particle volume concentration since only the forward compressional wave is considered as propagating beyond the region of a single isolated particle, and the effect of multiple particles is determined by the average superposition of their scattered fields.

However in the nonlinear model, the wave arriving at any particle is a combination of the incident wave together with all waves scattered by other particles. The resulting total scattered wave field is therefore a result of scattering of the incident wave by all particles and the rescattering (or multiple scattering) of already-scattered waves. All three wave modes (produced by scattering at a particle) contribute to the wave field at neighbouring particles, and can therefore be scattered by these neighbours, thereby producing compressional scattered waves as well as other modes. This effect creates a nonlinear concentration dependence of attenuation.

NOTE Multiple scattering depends on the configuration and aperture of the transducers as well as on the type of excitation signal, e.g. pulse, tone-burst, quasi-continuous, or continuous[20].

Multiple scattering models have largely considered only the multiple scattering of the compressional wave mode, neglecting the contribution of scattered thermal and shear waves to the wave field which is incident at a particle[11][12][13][14]. The second-order concentration effects obtained from these multiple scattering models are significant only where there is a substantial density difference between the phases. In many systems, the nonlinear effects due solely to compressional wave multiple scattering are small, and they can be modelled using the multiple scattering models mentioned above. Substantial nonlinear effects arise primarily because of the contributions of scattered thermal and shear waves to the incident field at any particle.

5.2 Concentration considerations

The distances over which thermal and viscous waves decrease by a factor of (1/e) are known as the thermal and viscous skin depths, respectively, which are calculated by Formulae (1) and (2). The skin depths for water are shown as a function of frequency in Figure 1.

$$\delta_T = \sqrt{\frac{2\kappa}{\rho C_P \omega}} \tag{1}$$

$$\delta_V = \sqrt{\frac{2\eta}{\rho\omega}} \tag{2}$$

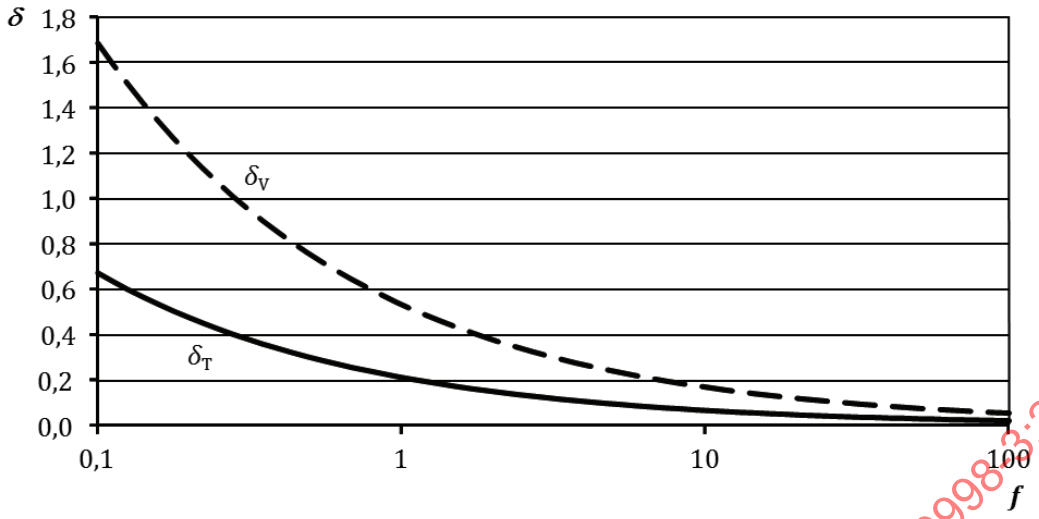

Key

δ skin depth (µm)

f frequency (MHz)

δ_V viscous wave skin depth

δ_T thermal wave skin depth

Figure 1 — Skin depth for viscous (dashed line) and thermal (solid line) waves in water at 20 °C

At high concentrations, the interparticle spacing may become small enough that the particles can no longer be considered to be completely isolated. This effect is compounded at low frequencies, where the skin depths calculated in Formulae (1) and (2) are longer. The thermal and shear waves produced by scattering at a particle contribute significantly to the wavefield at a neighbouring particle, being rescattered to produce compressional waves (and other modes). For practical purposes, the breakdown of linear theory (or nonlinear compressional models) occurs when the viscous or thermal waves from adjacent particles overlap significantly. Quantifying the overlap in simple terms is difficult, but a standard approach is to determine the concentration when the interparticle distance is less than or equal to the skin depth. Since the viscous layer has greater thickness in most liquids, the onset of multiple scattering occurs when the interparticle distance d equals the viscous skin depth.

For a suspension of monosized spheres, the interparticle distance d is given as a function of volume concentration ϕ[15] by

$$d = x\left[\left(\frac{\phi_m}{\phi}\right)^{1/3} - 1\right] \tag{3}$$

where

ϕ_m is the maximum volume concentration based on the packing arrangement;

x is the sphere diameter.

For random packing, ϕ_m typically has a value of approximately 0,6.

To determine conditions where consideration should be given to using a nonlinear model, Formulae (2) and (3) are combined to determine the concentration ϕ_{NL} at which the viscous skin depth becomes

equal to the interparticle distance. The resulting Formula (4) is expressed in terms of $x\sqrt{f}$ to produce a universal function:

$$d = \phi_m \left[\left(\sqrt{\frac{\eta}{\rho\pi}} \cdot \frac{1}{x\sqrt{f}} \right) + 1 \right]^{-3} \quad (4)$$

The results for aqueous slurries are shown in Figures 2 and 3; the calculations were done by assuming that ϕ_m = 0,6 and by substituting the viscosity and density of water.

For comparison, the calculation for slurries in hexadecane (a common solvent) is included as a broken line in Figure 2. The contour plot in Figure 3 repeats the calculation for water for explicit values of frequency and particle diameter.

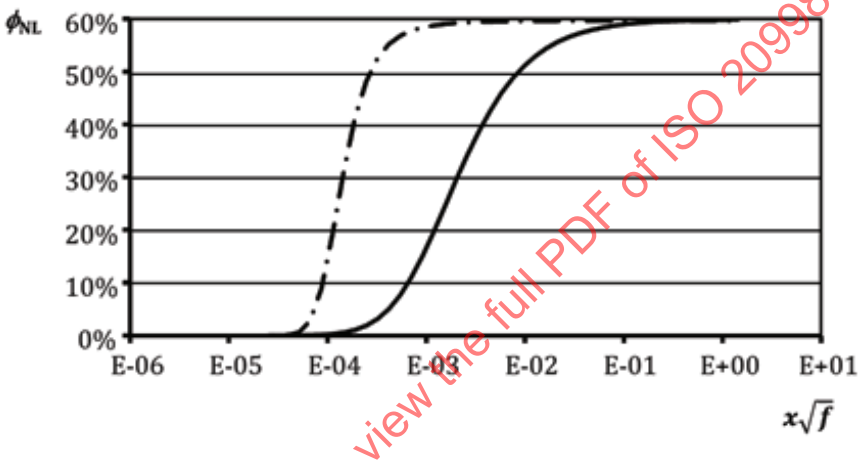

Key

ϕ_{NL} volume concentration at which nonlinear effects may become evident

$x\sqrt{f}$ product of particle size and square root of ultrasonic frequency (m·Hz½)

——— water

—.—. hexadecane

Figure 2 — Estimate of ϕ_{NL} (approximate concentration at which nonlinear effects may become evident) calculated for water and for hexadecane

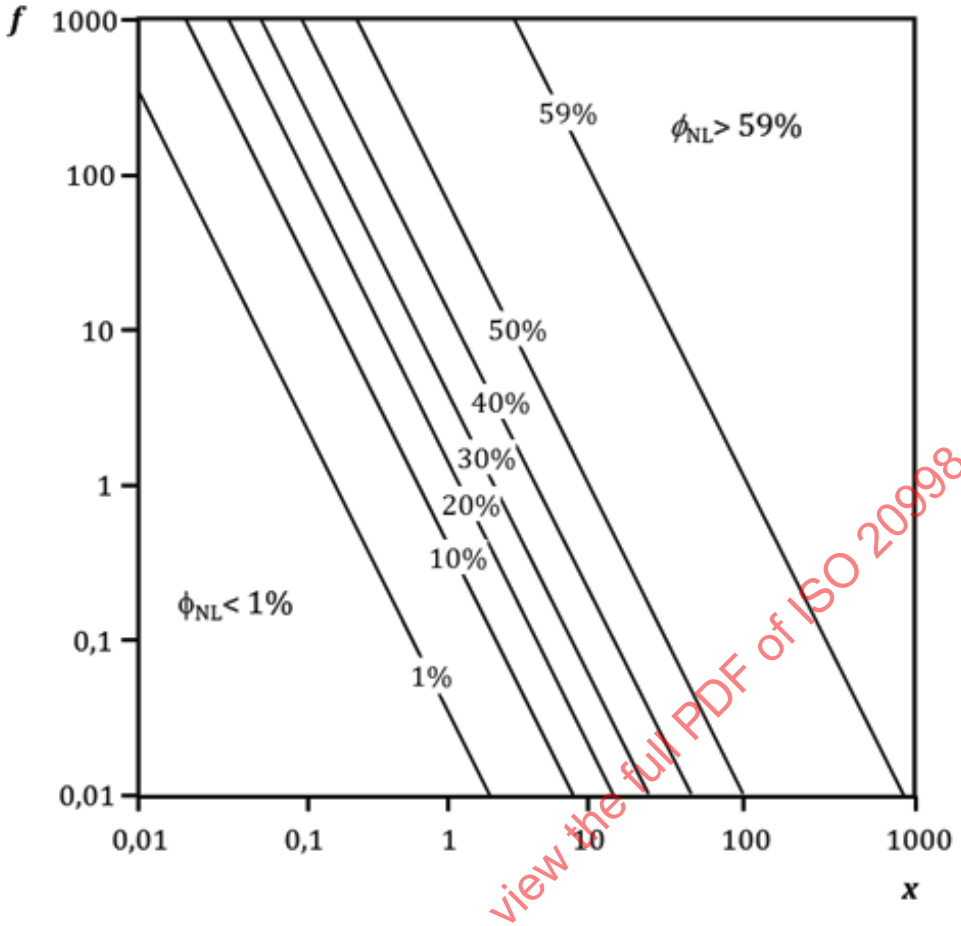

Key

f frequency (MHz)

x particle diameter (mm)

Figure 3 — Contour plot of ϕ_{NL} for water, as a function of frequency and particle diameter

As a practical example, consider a hypothetical ultrasonic spectroscopy system operating at frequencies in the range of 10 MHz to 100 MHz and measuring 0,1 µm diameter particles. The results shown in Figure 3 suggest that nonlinear effects should be considered at concentrations greater than a few volume percent. On the other hand, the same system could be used to measure particle size of 10 µm particles at concentrations of 50 % or more.

NOTE 1 Formula (4) and Figures 2 and 3 are provided only as a guideline for estimating ϕ_{NL}, the concentration limit beyond which the viscous wave interacts directly with neighbouring particles.

For concentrations in excess of ϕ_{NL}, the linear theories described in ISO 20998-2 may not be adequate for estimating particle size from measurements of the ultrasonic attenuation spectrum. In that situation, theories that predict a nonlinear relationship between attenuation and volume concentration (such as those described below) may be needed.

NOTE 2 Deviation from linear theory generally becomes greater with increasing concentration, decreasing frequency, or decreasing particle size.

5.3 Steric repulsion

Additional effects arise from the development of structure in the suspension due to steric exclusion of the particles, possibly augmented by hydrodynamic interaction forces and interactions of the

electrostatic double layers, or flocculation. Structure affects ultrasonic attenuation, and these effects have been studied extensively by Riebel et al.[16][17][18][19] The collective interaction of particles produces a "dependent scattering" contribution to the attenuation that is distinct from multiple scattering.[20]

6 Measurement issues in concentrated systems

6.1 General

The measurement of concentrated suspensions and emulsions may be complicated by difficulty in obtaining representative attenuation spectra. Commonly encountered issues and possible remedies are described below.

6.2 Path length limitation

In ultrasonic spectroscopy systems, the total attenuation (dB loss) in the received signal must be within the dynamic range of the instrument. The maximum path length between transmitting and receiving transducers is limited by the attenuation coefficient (dB/cm), which increases with concentration and frequency. Therefore, measurement of concentrated particle systems may require a shorter acoustic path length, which may not be practical depending on the application, or the use of a lower frequency range (if possible).

6.3 High attenuation

As the total attenuation increases, the signal-to-noise ratio (SNR) drops, and without some form of signal processing there will be a negative impact on data quality. A common signal processing technique is to average the result of many measurements of the attenuation spectrum. Another approach is to encode the transmitted ultrasound and to filter the received signals to reject those that do not correlate with the transmission.[21]

Bubble formation contributes to high signal attenuation and in some cases may block the ultrasonic signal completely.

6.4 Increased viscosity

For a given PSD, increasing particle concentration generally increases the viscosity of the slurry. Increased viscosity leads to several detrimental effects.

— First, bubbles become more prevalent and also more persistent once formed.

— Second, fluid flow is impeded in sensors with small transducer separation; two consequences are increased back-pressure in the sensor and particle segregation or exclusion within the flow.

— The third issue is the increased potential for transducer fouling, which necessitates frequent cleaning of the sensor.

In some applications, elevating the temperature might reduce the viscosity, but in general, it is preferable to minimize bubble formation, use a sensor with no constriction in flow, and provide for transducer cleaning if necessary.

6.5 Change in velocity

Sound velocity, which may change with particle concentration, affects ultrasonic propagation in three ways:

— First, group velocity determines the transit time between transducers.

— Second, changes to phase velocity can distort and broaden the waveform of an ultrasonic pulse. Without a feedback mechanism to adjust the timing and width of the time-domain signal capture, spectrometers that use a pulse technique might truncate the waveform. This feedback is generally provided via software.

— Finally, changes in sound velocity alter the wavelength and hence the diffraction field, thereby affecting the detected signal.

In order to measure concentrated suspensions, an ultrasonic spectrometer of any type shall be capable of adapting to changes in group and phase velocity.

6.6 Change in pulse shape

As noted above for instruments that are based on pulse techniques, changes in phase velocity will distort the shape of the received pulse. Additional distortion is caused by the frequency-dependent attenuation, which suppresses some frequency components more than others. This effect can also be seen in dilute suspensions.

6.7 Homogeneity

Agglomeration and flocculation become more prevalent at high concentration, which broadens the apparent PSD in the sample. Stirring or pumping may help to improve homogeneity temporarily.

7 Nonlinear attenuation

The observed ultrasonic attenuation spectrum, $\boldsymbol{\alpha}$, is dependent on the particle size distribution and on the particle concentration. In dilute suspensions and emulsions, the sound field interacts with each particle independently and the linear theories described in ISO 20998-2 are adequate for determining particle size. Some nonlinear dependence of attenuation on particle concentration results from multiple scattering of compressional waves, but these contributions are often small. However linear theories begin to fail in the case of emulsions when the thermal wavelength approaches or exceeds the interparticle spacing[10]. In cases dominated by visco-inertial effects, linear theories fail when the evanescent shear waves generated by mode conversion at one particle overlap with shear waves coming from another particle. In either case, the proximity of particles results in a nonlinear dependence of attenuation on concentration, and different theories are needed to determine particle size. A few examples are provided in Annex A; other theoretical models are reviewed in References [1], [2] and [10].

NOTE The term "scattering" is widely used to refer to the process by which all wave modes are produced at a particle.

8 Determination of particle size

8.1 Calculation

The mathematical methods described in ISO 20998-2:2013, 6.2 are recommended in conjunction with the nonlinear theories shown in Annex A to determine particle size distribution from observed ultrasonic attenuation data in concentrated systems. It is permitted to use empirical or semi-empirical calibration curves in place of these theories, provided the user qualifies the results as shown in Clause 9.

NOTE 1 Empirical and semi-empirical calibrations generally have a limited range of validity and can change suddenly as a result of physical changes in the system.

NOTE 2 Annex B provides one example of how to estimate PSD from an attenuation spectrum using the methods described in this document.

8.2 Limits of application

The typical particle size for ultrasonic analysis ranges from 10 nm to 3 mm, although particles outside this range have also been successfully measured. Measurements can be made for concentrations up to about 50 % by volume, depending on the density contrast between continuous and dispersed phases, the particle size and the frequency range. At the close packed limit where particle contacts become extensive, scattering models will break down due to the establishment of a frame modulus whereby acoustic propagation may occur through a continuum of particles that supports shear. At lower concentrations (see 5.2), the linear theories described in ISO 20998-2 are recommended.

The application of theoretical models requires the knowledge of the relevant model parameters, and empirical methods depend on correlations that may have limited applicability. Users should therefore be aware of possible changes in physical parameters, e.g. a variation of temperature or particle concentration that could affect the model.

9 Instrument qualification

9.1 Calibration

Ultrasonic spectroscopy systems are based on first principles. Thus, calibration in the strict sense is not required; however, it is still necessary and desirable to confirm the accurate operation of the instrument by a qualification procedure. See ISO 20998-1 for recommendations.

9.2 Precision

9.2.1 Reference materials

For testing precision, reference materials with an x_{90}/x_{10} ratio in the range of 1,5 to 10 should be used. It is desirable that reference materials used to determine precision are non-sedimenting and comprising spherical particles with diameters in the range of 0,1 µm to 1 µm. The reference material concentration shall be within 5 % of the volume concentration expected in the intended application.

9.2.2 Repeatability

The requirements given in ISO 20998-1 shall be followed. The instrument should be clean, and the liquid used for the background measurement should be virtually free of particles. Execute at least five consecutive measurements with the same dispersed sample aliquot or dispersed single shot samples. Calculate the mean and coefficient of variation (CV) for the x_{10}, x_{50}, and x_{90}. An instrument is considered to meet the requirements given in ISO 20998-1 for repeatability if the CV for each of the x_{10}, x_{50} and x_{90} is smaller than 10 %. If a larger CV value is obtained, then all potential error sources shall be checked.

9.2.3 Reproducibility

Reproducibility tests by different operators using different equipment shall follow the same measurement protocol as repeatability. At least three distinct samples of the same reference material shall be measured, and the mean and CV for the x_{10}, x_{50}, and x_{90} shall be calculated. A CV larger than that of repeatability may be expected due to differences in sampling or dispersion or between analysts or instruments. The certification for the reference material will contain information about the acceptable error for that material.

9.3 Accuracy

9.3.1 Qualification procedure

In the qualification step, the accuracy of the total measurement procedure is being examined. It is essential that a written procedure is available that describes sub-sampling, sample dispersion, the

ultrasonic measurement, and the calculation of the PSD in full detail. This procedure shall be followed in its entirety and the title and version number reported.

9.3.2 Reference materials

Certified reference materials (produced in accordance with ISO Guide 35) are preferred in the measurement of accuracy. These materials have a known size distribution of spherical particles with an x_{90}/x_{10} ratio in the range of 1,5 to 10. It is preferred that the median size of the certified reference material be chosen so that it lies within the size range contemplated for the end-use application. For single shot analysis, the full contents of the container shall be used. If sub-sampling is necessary, the sampling shall be done according to ISO 14488. If a protocol for sampling, dispersion or measurement is not available, the procedure that is used shall be reported with the final results.

9.3.3 Instrument preparation

The advice given in ISO 20998-1 should be followed. The instrument should be clean, and the liquid used for the background measurement should be free of particles.

9.3.4 Accuracy test

The written test protocol defined in 9.3.1 shall be followed for the accuracy test, which measures the PSD of the selected reference material. Single shot analysis may be applied. Analysis of sub-samples is permitted if the procedure for sub-sampling is also written and is documented to provide good repeatability. Analysis shall be made on five consecutive sample aliquots, and the average value and CV of the median size shall be calculated.

9.3.5 Qualification acceptance criteria

The expanded uncertainty stated for each certified size value of the standard reference material specification provides a set of maximum and minimum values that define the stated parameter. The qualification test shall be accepted if the resulting measured particles size distribution achieves both of the following criteria:

a) the reported average value of the median size measured in the qualification test is no smaller than 90 % of the minimum value and no larger than 110 % of the maximum value;

b) the reported CV of the median size does not exceed 10 %.

If a larger deviation is obtained, then all potential error sources should be checked. If it is not possible to meet the qualification criteria of this clause, then this failure shall be noted on the final PSD report.

If a higher standard of accuracy is required for any reason, then a reference material should be chosen with a narrow confidence interval and a total protocol for sampling, dispersion and measurement should be used that guarantees minimum deviation.

10 Reporting of results

The particle size distribution results shall be reported according to the guidelines in ISO 20998-1:2006, Clause 6.

Annex A
(informative)

Theories of attenuation in concentrated systems

A.1 Scattering models

A.1.1 Multiple scattering

The scattering models discussed in the linear theory part (ISO 20998-2) considered only the cumulative energy loss due to scattering and absorption at individual particles. Thus, the total loss is proportional to the number density of particles, and the wave field that arrives at any one particle is defined as equivalent to the incident wave. In a multiple scattering model, the wave field which is experienced by any particle is considered to consist of the incident (driving) wave *and* the waves scattered by all other particles. This net wave field then results in a scattered wave from that particle which itself contributes to the wave field at neighbouring particles. The combined scattered wave field takes the form of a coherent wave once averaging over all particle locations has been effected. It is the wavenumber of this coherent wave which characterizes compressional wave propagation through a dispersion (incorporating coherent averaging).

NOTE Multiple scattering can occur at high concentration and also for a sufficiently long path length.

Multiple scattering models have focused on the compressional wave mode, and in most cases include only the contribution of scattered *compressional* waves by neighbouring particles. Thermal and shear waves are assumed to decay close to the particle and have no influence on nearby particles. While Foldy[22] is an early example of a multiple scattering model, the most widely accepted forms are those of Lloyd and Berry[11] (originally derived for electromagnetic waves) and Waterman and Truell[12]. The Lloyd and Berry formula was confirmed by Linton and Martin[14] for the acoustic case. Waterman later corrected an approximation in their model[13]; the later model is equivalent to the Lloyd and Berry model to second order in concentration. The multiple scattering models are expressed as a wavenumber for compressional waves through the dispersed medium, in terms of scattering coefficients at the individual particles (these are often called the transition factor or operator). These scattering coefficients can be derived using models such as ECAH for the single particle scattering case. A more extensive review and simplified versions of the models can be found in Challis et al.[10]

The original multiple scattering models were derived only for monodisperse systems. Two alternative adjustments have been proposed to incorporate the effects of polydispersity, although neither has been rigorously derived from multiple scattering theory. That of Povey[2] defines a single-particle scattering coefficient that is averaged (volume-fraction-weighted) over all particle sizes, whereas Challis et al.[10] propose a summation over particle size in the wavenumber expression. The former method accounts for scattering from particles of any size combination. The two versions are equivalent to first order in concentration.

Multiple scattering models that include the effects caused by thermal and shear wave overlap are few, and are either proprietary or in development. Alba[23] formulated a generalized model for multiple scattering of all three wave modes, implementing a numerical solution that has been validated for particle sizing for a number of systems. More recently, Luppé et al. [24] addressed the same problem, deriving a modification to the Lloyd/Berry nonlinear wavenumber with additional scattering contributions due to thermal and shear wave effects; but their model has yet to be validated by application to measurements.

A.1.2 Core-shell/effective medium scattering

Core-shell models have been developed in order to account for the nonlinear dependence of attenuation on concentration caused by thermal and shear wave overlap. These long-wavelength models (see Figure A.1) treat each individual particle with radius a as being embedded in a shell, with radius M, of the suspending medium. The shell is surrounded by a homogeneous medium that has some averaged or effective properties of the dispersion as a whole. The existence of the shell, the surface at which boundary conditions (in temperature, heat flux, displacement, stress etc.) are applied, enables the influence of neighbouring particles on the wave field at the particle to be included on an averaged basis. Hemar et al.[25] constructed a core-shell model for the thermal wave problem (neglecting viscous absorption) based on a derivation of thermal absorption by Isakovich.[26] This model has much in common with the coupled phase approach discussed in the next clause. Later, McClements et al.[27] [28] combined these approaches into a multiple scattering model, accounting for the nonlinear compressional wave effects (through the standard Lloyd/Berry terms), thermal wave overlap, and viscous absorption (but not shear wave overlap effects). Their result is expressed as an analytical modification factor to the single-particle scattering coefficients obtained by ECAH (see ISO 20998-2).

Hipp et al.[29] applied the core-shell principle to the ECAH analysis of the single-particle scattering coefficients. By using effective medium properties outside the shell, and applying appropriate boundary conditions, they derived an effective scattering coefficient which incorporates averaged influences of neighbouring particles, for all three wave modes, compressional, thermal and shear. The resulting coefficient is used in the Lloyd/Berry multiple scattering model[11] to obtain an effective wavenumber for the dispersion. The model is equivalent to the Anson and Chivers model[30] for a particle with a physical shell (such as an oil-filled aluminium sphere), but differs in the selected scattering coefficient for use in the multiple scattering wavenumber. The Hipp model is the most comprehensive core-shell model available.

When compared with experimental data, the core-shell models have shown a high degree of success. However, they do suffer from some difficulties for particle sizing, principally in the definition of the shell radius in a polydisperse system. The models were derived only for monodisperse systems, and no formal extension to polydisperse systems has been obtained. The shell radius is generally taken to be such that the concentration of particle inside the shell is equivalent to that of the dispersion as a whole. For a polydisperse system, this could mean using a different shell radius for each size of particle, or a single shell definition which could be smaller than the largest particles. The definition of the properties outside the shell is also subject to debate. Although the core-shell models appear to be of high quality for monodisperse systems, these difficulties render them unsuitable for particle sizing applications in system with a broad particle size distribution.

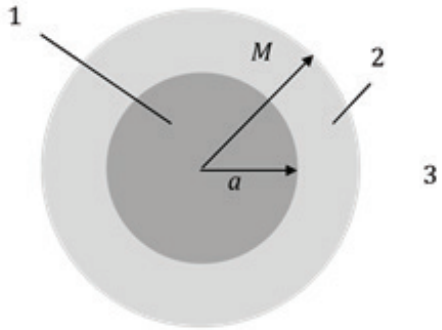

Key

1 particle
2 pure continuous phase
3 effective medium
a particle radius
M shell radius

Figure A.1 — Core-shell model

A.2 Coupled-phase models

Coupled phase models treat the dispersion as a volume-averaged continuum, an assumption which is valid in the very long wavelength region. The principles of conservation of mass and momentum (and energy, where thermal contributions are included) are applied to the two phases; coupling between the phases occurs through terms defining viscous drag (and heat transfer where thermal contributions are included). The acoustic wavenumber is derived from wave solutions to the conservation equations.

Coupled phase models have largely focused on the hydrodynamically-mediated shear wave overlap problem. In these models, the principal component of the model is in the viscous drag coupling term for a particle in a concentrated dispersion, often expressed through a concentration-dependent viscosity. An extensive literature exists on such viscosity/viscous-drag models[10][31]. Many of these hydrodynamic studies have adopted a form of core-shell model, described earlier, in which a variety of boundary conditions have been chosen at the shell boundary. The early coupled-phase model by Harker and Temple[32] adopted the Vand viscosity model[33] for the viscous drag term, whereas Strout[31] used a modified form of the Happel model[34], which is also used by Dukhin and Goetz[1]. Later coupled-phase models incorporated the contributions of thermal wave overlap through a similar core-shell model for the heat transfer terms. In fact, the thermal core-shell analysis used by Evans and Attenborough[35] is equivalent to the core-shell model of Hemar et al.[25], described in the previous clause, which was used as the precursor to the scattering core-shell model.

Evans and Attenborough's coupled phase model includes both viscous and thermal wave interactions in concentrated systems[35]. In common with other coupled phase theories, it assumes wavelengths that are large compared with the scattering particles, and is accurate only up to dimensionless radii of typically 0,01. Coupled phase models were originally derived only for the monodisperse case, but extensions for polydisperse systems have been proposed[36] [37] [38]. Annex B provides an example of a coupled phase model and its application.

Annex B
(informative)

Practical example of PSD measurement (coupled phase model)

B.1 Introduction

The purpose of this annex is to provide one example of how to estimate PSD from an attenuation spectrum using the methods described in this document. This example uses the "Solver" tool in Microsoft Excel[1)] to perform the inversion. A similar approach to inverting the ultrasonic data is demonstrated in ISO 20998-2:2013, Annex F for the case of a dilute suspension.

NOTE The example given here is for the purpose of demonstration only. Other specimens within the scope of this document can be measured, provided a suitable attenuation model is used in the inversion of the observed attenuation spectra; other inversion techniques could be used.

B.2 Attenuation spectrum

This example uses the attenuation spectrum of alumina in water at a solids concentration of 10 % by volume. The data shown in Figure B.1 was measured on a Dispersion Technology (Bedford Hills, NY) model 1200 spectrometer and closely matches the data published previously by Takeda and Goetz[39]. The alumina (Sumitomo Chemical AKP-30) was mixed into 0,2 wt% sodium hexamataphosphate aqueous solution and then sonicated for 1 min at an ultrasonic power of 145 W. Discrete values are shown in Table B.1 for convenience in subsequent calculations.

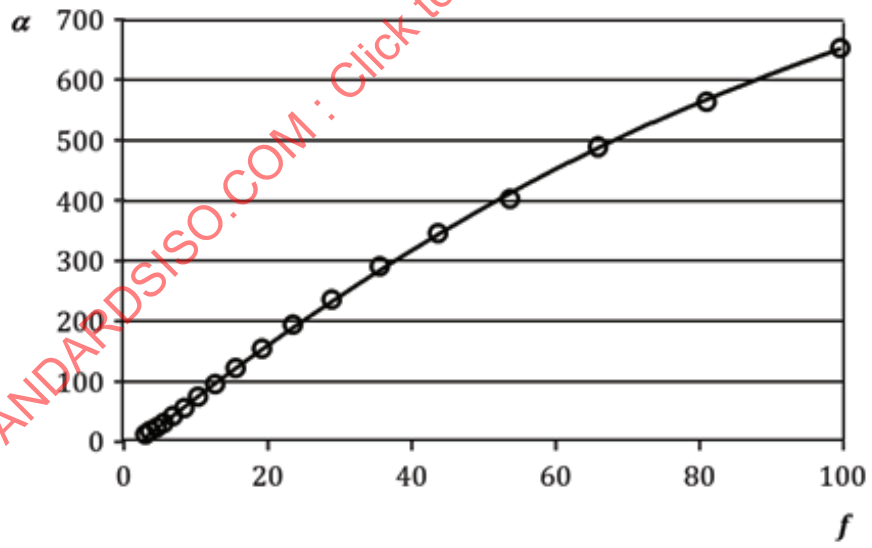

Key

α attenuation (dB/cm)

f frequency (MHz)

Figure B.1 — Attenuation spectrum of 10 vol% alumina in water

1) Excel is the trade name of a product supplied by Microsoft. This information is given for the convenience of users of this document and does not constitute an endorsement by ISO of the product named. Equivalent products may be used if they can be shown to lead to the same results.

Table B.1 — Observed attenuation data for 10 vol% AKP-30 alumina in water

Frequency (MHz)	**Attenuation** (dB/m)
3	11,728
3,686	16,529
4,529	22,483
5,565	31,053
6,838	42,493
8,402	55,218
10,324	74,801
12,685	95,53
15,586	122,619
19,151	153,08
23,532	193,792
28,914	234,986
35,527	290,833
43,653	344,715
53,637	401,735
65,905	488,964
80,979	563,609
99,5	653,738

The PSD measured via laser diffraction with a Horiba LA-960 for a dilute suspension is shown for reference in Table B.2 below. The reported x_{50} is 0,199 µm.

Table B.2 — Laser diffraction PSD for alumina sample

Size (µm)	**Differential volume fraction** (%)	**Cumulative volume fraction** (%)	**Size** (µm)	**Differential volume fraction** (%)	**Cumulative volume fraction** (%)
0,051	0,000	0,000	0,445	3,899	89,753
0,058	0,556	0,556	0,510	2,718	92,471
0,067	1,202	1,758	0,584	1,856	94,326
0,076	2,212	3,970	0,669	1,282	95,608
0,087	3,33	7,300	0,766	0,922	96,530
0,100	4,317	11,617	0,877	0,704	97,233
0,110	5,471	17,088	1,005	0,576	97,809
0,131	6,735	23,823	1,151	0,517	98,326
0,150	7,837	31,660	1,318	0,458	98,785
0,172	8,64	40,299	1,510	0,382	99,166
0,193	9,039	49,338	1,729	0,304	99,470
0,226	8,958	58,296	1,981	0,234	99,705
0,259	8,372	66,668	2,269	0,173	99,878
0,296	7,446	74,114	2,599	0,123	100,000
0,339	6,446	80,560	2,976	0,000	100,000
0,389	5,294	85,854			

Referring to Figure 3 in 5.2, it is evident that 0,2 µm particles in water at 10 vol% concentration are expected to have nonlinear attenuation. Therefore, the viscous loss model discussed in

ISO 20998-2:2013, Annex F is not suitable for this application; instead, a coupled phase model has been chosen for this example.

B.3 Coupled phase model

The coupled phase model considers the dispersed system as a mixture of two phases, with an effective density and compressibility are defined for the mixture[32]. The length scales are such that the mixture can be treated as volume averaged continuum such that $ka < 1$. The most basic form of the model treats only visco-inertial loss mechanisms and should be appropriate for physical systems with a large density contrast between the particles and continuous medium.

Under these assumptions, the square of the effective wavenumber of the forward scattered wave is given in Formula (B.1)[32]:

$$k^2 = \frac{\omega^2 \bar{\beta}\rho\left[\rho'\left(1-\phi+\phi S\right)+\rho S\left(1-\phi\right)\right]}{\rho'\left(1-\phi\right)^2+\rho\left[S+\phi\left(1-\phi\right)\right]} \tag{B.1}$$

with the mean compressibility given by Formula (B.2):

$$\bar{\beta} = \phi\beta' + \left(1-\phi\right)\beta \tag{B.2}$$

where

$$\beta = \frac{1}{c^2\rho} \tag{B.3}$$

$$\beta' = \frac{1}{\left(c'\right)^2\rho'} \tag{B.4}$$

The factor S is a complex number representing the effective coupling between fluid and particle:

$$S = G + iR \tag{B.5}$$

with the definitions

$$G = \left(\frac{1}{2}\right)\cdot\frac{1+2\phi}{1-\phi} + \frac{9\delta_V}{4a} \tag{B.6}$$

$$R = \frac{9\delta_V}{4a}\left(1+\frac{\delta_V}{a}\right) \tag{B.7}$$

The thickness δ_V is defined in Formula (2).

The expression for k^2 shown in Formula (B.1) can be simplified by defining

$$\bar{\rho} = \rho'\phi + \rho\left(1-\phi\right) \tag{B.8}$$

$$\rho^* = \rho'\left(1-\phi\right) + \rho\phi \tag{B.9}$$

These quantities correspond to the mean density of the slurry at the specified concentration ϕ and at the complementary concentration (1–ϕ), respectively. With these definitions, Formula (B.1) can be rewritten as

$$k^2 = \frac{\omega^2 \bar{\beta}\rho\left[\rho'\left(1-\phi\right) + \bar{\rho}S\right]}{\rho^*\left(1-\phi\right) + \rho S} \tag{B.10}$$

Attenuation is defined to be the imaginary part of the wavenumber k, so α can be determined from Formula (B.10) by computing the imaginary component of k^2:

$$\alpha = \frac{c}{2\omega} \cdot \mathrm{Im}\left(k^2\right) \tag{B.11}$$

Combining Formulae (B.10) and (B.11) yields

$$\alpha = \left(\frac{\omega c \bar{\beta}\rho}{2}\right) \cdot \frac{\left(\rho^*\bar{\rho} - \rho'\rho\right)\left(1-\phi\right)R}{\left[\rho^*\left(1-\phi\right) + \rho G\right]^2 + \left(\rho R\right)^2} \tag{B.12}$$

NOTE Technically, Formula (B.12) is derived for slurry that contains monodisperse particles. For the explicit solution to polydisperse suspensions, see Reference [40].

B.4 PSD model

Assuming that the volume-weighted PSD can be described as a log-normal distribution, then the volume fraction between sizes x_{n-1} and x_n is given by

$$\phi_n = Q_3\left(x_n\right) - Q_3\left(x_{n-1}\right) \tag{B.13}$$

The cumulative log-normal distribution $Q_3(x)$ can be calculated by the built-in function *lognormdist.*

NOTE 1 In order to conform to the definitions used here, the correct function call is LOGNORMDIST(x,LN(x_{50}),s).

NOTE 2 The Geometric Standard Deviation (GSD) of the PSD is equal to *exp(s)*.

In the example shown in Table B.3, a set of 41 logarithmically-spaced particle diameters is defined in Column A: {x_1 = 1,00 × 10^{-8} m; x_2 = 1,20 × 10^{-8} m; x_3 = 1,44 × 10^{-8} m, …, x_{41} = 1,47 × 10^{-5} m}. These diameters define a set of 40 size intervals (i.e. size classes) where the average particle size X_n of the nth class is the geometric mean:

$$X_n = \sqrt{x_{n-1}x_n} \tag{B.14}$$

Using an arbitrary initial guess of x_{50} = 1 × 10^{-7} m and s = 0,40, the trial cumulative PSD is calculated in Column B using the *lognormdist* function to evaluate $Q_3(x_n)$ at each particle size. The set of {ϕ_n} is determined from Formula (B.13) in Column C, and the geometric mean diameter of each size class in Column D is calculated from Formula (B.14).

Table B.3 — Partial listing of initial entries in the spreadsheet

	A	B	C	D
1	x	P(x)	vol fraction	GM diameter
2	1,00E-08	0,0000		
3	1,20E-08	0,0000	5,34E-08	1,095E-08
4	1,44E-08	0,0000	5,76E-07	1,315E-08
5	1,73E-08	0,0000	5,06E-06	1,577E-08
6	2,07E-08	0,0000	3,62E-05	1,893E-08
7	2,49E-08	0,0003	2,11E-04	2,272E-08
8	2,99E-08	0,0013	1,00E-03	2,726E-08
9	3,58E-08	0,0051	3,89E-03	3,271E-08
10	4,30E-08	0,0174	1,23E-02	3,925E-08
11	5,16E-08	0,0490	3,16E-02	4,710E-08
12	6,19E-08	0,1154	6,63E-02	5,652E-08
13	7,43E-08	0,2289	1,13E-01	6,783E-08
14	8,92E-08	0,3871	1,58E-01	8,139E-08
15	1,07E-07	0,5671	1,80E-01	9,767E-08
NOTE The sum of Column C over all 40 values must be equal to 1.				

B.5 Inversion

Following the scheme outlined in ISO 20998-2:2013, Annexes D and F, one can use the coupled phase model [Formula (B.12)] to estimate the attenuation spectrum expected from the trial PSD. The physical constants used in this calculation are listed in Table B.4.

Table B.4 — Physical constants for alumina in water example

ϕ	0,1
ρ	997 kg/m^3
ρ'	3970 kg/m^3
c	1497 m/s
c'	7776 m/s
η	8,91E-04 Pa s

Table B.5 shows a portion of the spreadsheet used for this calculation. The mean radius in Row 7 is one-half of the diameters transposed from Column D in Table B.3, and Row 8 is the transpose of Column C in Table B.3. Columns F and G contain the measured attenuation spectrum from Table B.1.

Table B.5 — Partial listing of entries in the spreadsheet

	F	G	H	I	J	K
7			mean radius:	5,477E-09	6,573E-09	7,887E-09
8			vol fraction:	5,340E-08	5,758E-07	5,059E-06
9						
10	**freq** (MHz)	**α expt** (dB/cm)	**α model** (dB/cm)	**Weighted attenuation**		
11	3,00	11,73	4,29	2,617E-09	4,049E-08	5,100E-07
12	3,69	16,53	6,24	3,943E-09	6,098E-08	7,677E-07
13	4,53	22,48	9,03	5,940E-09	9,182E-08	1,155E-06

Table B.5 *(continued)*

	F	G	H	I	J	K
14	5,57	31,05	12,98	8,946E-09	1,382E-07	1,738E-06
15	6,84	42,49	18,54	1,347E-08	2,080E-07	2,614E-06
16	8,40	55,22	26,30	2,028E-08	3,129E-07	3,929E-06
17	10,32	74,80	37,01	3,051E-08	4,705E-07	5,903E-06
18	12,69	95,53	51,64	4,589E-08	7,072E-07	8,863E-06
19	15,59	122,62	71,40	6,899E-08	1,062E-06	1,330E-05
20	19,15	153,08	97,76	1,037E-07	1,595E-06	1,994E-05
21	23,53	193,79	132,48	1,557E-07	2,393E-06	2,988E-05
22	28,91	234,99	177,58	2,338E-07	3,587E-06	4,472E-05
23	35,53	290,83	235,39	3,507E-07	5,373E-06	6,687E-05
24	43,653	344,715	308,44	5,256E-07	8,041E-06	9,987E-05
25	53,637	401,735	399,46	7,872E-07	1,202E-05	1,489E-04
26	65,905	488,964	511,31	1,178E-06	1,795E-05	2,218E-04
27	80,979	563,609	646,86	1,760E-06	2,676E-05	3,296E-04
28	99,5	653,738	808,96	2,627E-06	3,982E-05	4,889E-04

The attenuation coefficient at a given frequency is the sum of contributions from each size class, weighted by the corresponding volume fraction. For example, cell J11 in Table B.5 is calculated by multiplying the volume fraction in J8 by the attenuation predicted by Formula (B.12) for the particle radius shown in cell J7 at the frequency shown in cell F11, at the stated volume concentration of 10 %. If the concentration is unknown, it may be used as a free parameter in the fitting procedure. The expected attenuation at 3 MHz, shown in cell H11, is the sum of the cells in the range I11:AV11 (row 11), and the results for other frequencies are calculated in rows 12-28. Predicted attenuation values in column H are compared with the measured attenuation spectrum shown in column G by calculating the root mean square (RMS) error:

$$E_{\mathrm{RMS}} = \sqrt{\frac{1}{N}\left[\sum_{n=1}^{N}\left(G_n - H_n\right)^2\right]} \tag{B.15}$$

Using the "Solver" tool in the spreadsheet, the error signal is minimised by adjusting the values of x_{50} and s (and also ϕ in cases where the concentration is unknown), subject to the constraint that they remain positive. An effective scheme is to adjust x_{50} (holding s constant) first, then to adjust s (holding x_{50} constant), then to adjust both values simultaneously. After Solver converges on a solution, the PSD can be read from Columns A and B (cumulative distribution) or Columns D and C (differential distribution) as described in B.4.

B.6 Results

In this example, the solver converged on $x_{50} = 2{,}234 \times 10^{-7}$ m and $s = 0{,}404$. The fitted attenuation model and the measured attenuation spectrum are compared in Figure B.2 and Table B.6. For comparison, Figure B.2 includes a calculation of the attenuation from the viscous loss model using the same PSD and concentration.